PCCP

Pairing of the nucleobase guanine studied by IR–UV double-resonance spectroscopy and *ab initio* calculations

Eyal Nir,[a] Christoph Janzen,[b] Petra Imhof,[b] Karl Kleinermanns[b] and Mattanjah S. de Vries[c]

[a] *Department of Chemistry, The Hebrew University, Jerusalem 91904, Israel*
[b] *Institut für Physikalische Chemie und Elektrochemie I, Heinrich Heine Universität Duesseldorf, 40225 Düsseldorf, Germany*
[c] *Department of Chemistry and Biochemistry, University of California, Santa Barbara, California 93106, USA*

Received 12th November 2001, Accepted 22nd November 2001
First published as an Advance Article on the web 29th January 2002

In this paper we present detailed R2PI spectra with IR–UV and UV–UV double resonance measurements of the guanine dimer (GG) and its methylated derivatives. We show that there are two isomers of GG in the investigated wavelength range from 32565 to 33600 cm^{-1}. We were able to assign the two isomers to specific structures based on comparison of the intermolecular vibronic patterns of the dimers with and without methylation, on analysis of the IR spectra in the range of the OH and NH stretching vibrations and on comparison with *ab initio* calculated dimer stabilities and vibrational frequencies. In both structures both guanine moieties are in the keto tautomeric form, even though the enol tautomers are also present in the beam. One isomer exhibits nonsymmetric hydrogen bonding with HNH···N, NH···N and C=O···HNH interactions (K9K7-2). The other isomer has a symmetrical hydrogen bond arrangement with C=O···NH/NH···O=C bonding (K9K7-1). The most stable guanine dimer forms C=O···NH/NH···O=C hydrogen bonds and has C_{2h} symmetry (K9K9-1). Due to its strong exciton splitting the allowed S_0–S_2 transition is outside the investigated spectral range. We did not observe any keto–enol or enol–enol dimers in the investigated wavelength region. The calculations predict these dimers to be considerably less stable.

I Introduction

In addition to the usual Watson–Crick base pairs in DNA, there exist less common base pairs that are important in RNA structure and in nucleic acid replication and transcription, especially in tRNA. One of these rare pairs is the guanine dimer G–G. This base pair plays an important role in telomers which are special structures at the end of linear eucaryotic chromosomes.[1,2] The guanine molecules at the end of the telomer fold into a hairpin *via* G–G base pairing, the end of which acts as primer for the synthesis of the complementary DNA strand.[3] It has been speculated that the gradual loss of guanine from telomers is a key process in aging. G–G base pairs also play a role in specific recognition mechanisms.[4] From calculations it is well known that the stability of G–G base pairs is similar to that of the usual G–C base pair and, in fact, considerably more stable than that of the usual A–T base pair.[5–7] We have recently reported mass selected vibronic spectra of G–G dimers as isolated clusters in a supersonic jet.[8] Jet spectroscopy makes it possible to study interactions between molecules in the absence of external effects such as solvent interactions, crystal modes and collective modes of the DNA backbone. By employing UV–UV double resonance spectroscopy we identified contributions to the vibronic spectrum from two isomers of G–G, but we did not assign the two spectra to definite cluster structures. In the following we present detailed IR–UV double resonance measurements of the guanine dimer and its methylated derivatives, which now provide the necessary information for structure assignment. From our measurements of the guanine monomer we know that three tautomers (9H- or 7H-enol, 9H-keto, 7H-keto) are abundant in our jet experiment, thus making possible a large number of potential dimer configurations.[9] In particular, the comparison of the infrared spectra obtained from the IR–UV experiments with *ab initio* calculated frequencies for the different cluster structures including the methylated ones enables us to assign the two isomers to definite cluster structures.

II Experimental and theoretical methods

The measurements were performed with an apparatus described in detail elsewhere.[10] In short, material is laser desorbed from a graphite sample in front of a pulsed nozzle. Typical fluences of the Nd:YAG desorption laser operated at 1064 nm (where graphite absorbs but guanine does not) are about 1 mJ cm^{-2} or less, which is considerably lower than the fluences normally used for ablation. The laser is focused to a spot of about 0.5 mm diameter within 2 mm in front of the nozzle. We used a pulsed valve (General Valve; Iota One) with a nozzle diameter of 1 mm at a backing pressure of about 5 atm argon or CO_2 drive gas. The ionization lasers cross the skimmed molecular beam at right angles inside the source region of a reflectron time-of-flight (TOF) mass spectrometer. By monitoring the mass peak of guanine dimers at $m/z = 302$ while varying the two photon, one color ionization wavelength, we obtain resonant two photon ionization (R2PI) mass selected excitation spectra. We perform spectral hole burning (SHB) by using two counterpropagating dye laser pulses with a delay of about 150 ns. This generates two peaks in the TOF spectrum – the first from the "burn" laser and the second from the "probe" laser. When both lasers are tuned to a resonance of the same isomer, the burn laser causes a decrease in the signal of the probe laser.[11–15] We scan the burn laser while the probe

 DOI: 10.1039/b110360c

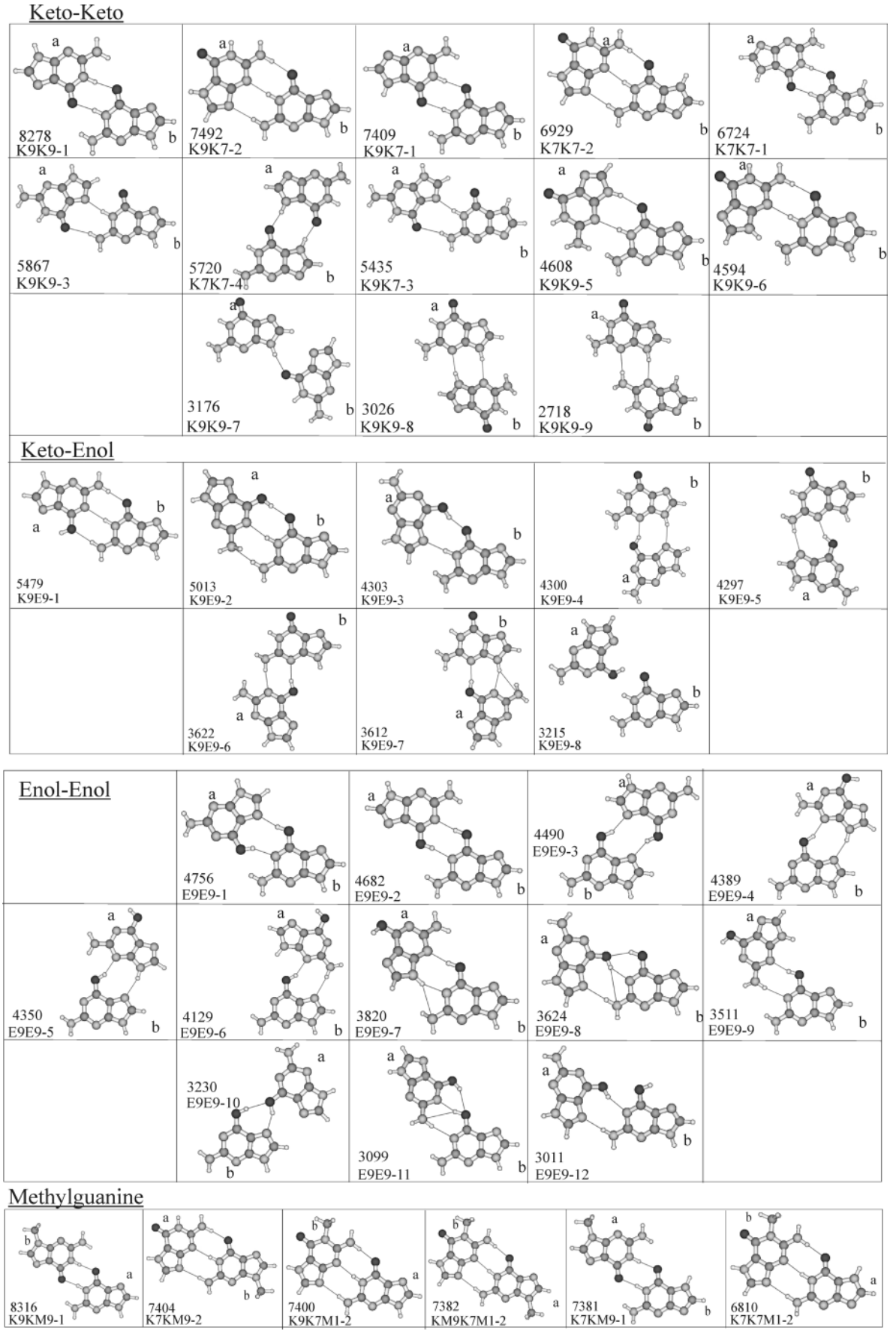

Fig. 1 Structures and stabilities of the most stable guanine–guanine isomers and methylguanine dimers calculated at the HF/6-31G(d,p) level with ZPE included. K and E denote the keto or enol tautomer of guanine, 9 and 7 the position of H substitution, M indicates methyl substitution and −1, −2... associates clusters with the same H bond arrangement and orders these cluster families according to their stability. For example K9K9-1 labels the 9H-keto −9 H-keto dimer with CO···NH/NH···O=C bonding which is the most stable cluster in this family of H bond arrangements (and altogether the most stable one). The numbers in the figures are the cluster dissociation energies (cm^{-1}) with ZPE included.

laser frequency is fixed to an intense band of one isomer. If a significant band of the R2PI spectrum is missing in the burn spectrum it belongs to another isomer (or to a hot band, which however we do not observe in our guanine spectra). In the next step we probe at this frequency while scanning the pump laser to reveal the spectrum of the next isomer.

We perform IR–UV SHB with the same method but taking a difference frequency IR laser as burn laser. The radiation from an infrared dye (a mixture of Styryl 8 and Styryl 9) is aligned collinearly with the perpendicularly polarized ND:YAG fundamental (1064 nm) and directed through a MgO-doped $LiNbO_3$ crystal to generate 3300–4000 cm^{-1} tunable IR light. Suitable dielectric mirrors separate the ND:YAG fundamental and the dye laser beam behind the crystal. We typically use 50 mJ of the YAG fundamental and 10 mJ of the dye laser to obtain around 1 mJ $pulse^{-1}$ IR radiation between 3300 and 4000 cm^{-1} with a bandwidth of <0.1 cm^{-1}. The IR laser is calibrated by recording a water vapor spectrum. Color centers in the $LiNbO_3$ crystal lead to a decrease in the IR intensity from 3515 to 3550 cm^{-1}. In that spectral range we use another $LiNbO_3$ crystal with a gap in another region. The IR laser power below 3300 cm^{-1} was too low to perform reliable experiments.

The calculations have been carried out using the Gaussian 98 program package.[16] We performed Hartree–Fock (HF) calculations utilizing a 6-31G(d,p) basis set. All structures were fully optimized on this level with 10^{-8} E_h as the SCF convergence criterion and 1.5×10^{-5} E_h a_0^{-1} and E_h $degree^{-1}$, respectively, as convergence criteria for the gradient optimization of the structures. The vibrational frequencies were obtained by performing a normal mode analysis on the optimized geometries using analytical gradients of the energy. The binding energies of the cluster were corrected for zero point energy (ZPE) at the HF-level. We also performed basis set superposition error (BSSE) corrections for some of the clusters but noticed that the order of cluster stability was generally not changed by including this correction. In order to estimate transition dipole moments we performed calculations with the time dependent density functional method (TD-DFT) on the HF-optimized structures of the clusters K9K9-1, K9K7-1 and K9K7-2. We used the B3LYP functional provided by the Gaussian program package and the 3-21G, 6-31G(d,p) and 6-311++G(d,p) basis sets to check for independence of our results from the size of the basis set.

III Results

Calculated structures

Fig. 1 displays the structures of the most stable guanine–guanine (GG) isomers obtained from calculations at the HF/6-31G(d,p) level. We obtained the initial structures for geometry optimization by circling one guanine molecule around the other guanine molecule and searching for possible hydrogen bond interactions. We repeated this procedure with the stationary guanine molecule turned over. Attempts to obtain GG "sandwich" structures with stability comparable to the most stable hydrogen bonded structures failed. This is as expected because the inclusion of electron correlation is needed to obtain stable stacked structures. Electron correlation is lacking in the HF calculations. Calculations including this effect have however shown that the strongly H bonded GG structures are generally far more stable than the stacked ones.[7,17] From our previous IR–UV experiments with guanine monomers we know that three guanine tautomers are abundant in the jet, namely 7H- or 9H-enol and 9H-/7H-keto guanine. A fourth tautomer may be present as well with less abundance.[18] We therefore optimized all possible structures for each of the 6 combinations of these three major tautomers, which led to a total of 39 different stable structures. To distinguish different structures we adopt a notation of the form $X_1N_1X_2N_2$-*I*, where X_i is either E or K, denoting the enol or keto tautomer, and N_i is either 7 or 9, denoting the 7H or 9H tautomer, respectively. *I* is a number to distinguish different structures for the same tautomer combination.

Fig. 1 and Table 1 list the structures ranked by stabilization energy, which is defined as

$$D_0 = D_e(\mathrm{cl}) - D_e(\mathrm{mA}) + D_e(\mathrm{mB}) + \mathrm{ZP}(\mathrm{cl}) - \mathrm{ZP}(\mathrm{mA}) + \mathrm{ZP}(\mathrm{mB}),$$

in which D_e denotes the electronic dissociation energy at the HF/6-31G(d,p) level, ZP denotes zero point vibrational energy, and cl, mA, and mB denote the cluster, monomer A and monomer B, respectively. According to our calculations the GG dimer K9K9-1 with a symmetrical C=O···NH/NH···O=C bonding is the most stable structure. It exhibits C_{2h} symmetry. K7K7-1 is considerably less stable. The mixed dimers consisting of 9H- and 7H-keto tautomers of guanine as cluster moieties with HNH···N, NH···N and O=C···HNH interactions (K9K7-2), the same H bond arrangement with 7H-/7H-keto moieties (K7K7-2) and K9K7-1 show similar stability. K9K9-2 with an H atom in position 9 allows no HNH···N9 hydrogen bonding and therefore no structure 2. All other keto–keto, keto–enol and enol–enol clusters have much smaller stabilization energies and can be studied in Fig.1 together with the most stable methylguanine isomers.

Fig. 2 shows the intermolecular vibrational frequencies of K9K7-1 calculated at the HF/6-31G(d,p) level and their atomic elongations: butterfly, torsion and gearing of the two rings, antisymmetric out-of-plane bending (step motion of the two moieties), antisymmetric stretch (in-plane bending of the two monomer moieties) and symmetric stretch vibrations. These six intermolecular vibrations originate from the three

Table 1 Dissociation energies D_0 (in cm^{-1}) of the most stable guanine dimer structures obtained by correcting the electronic dissociation energy (D_e) at the HF/6–31G(d,p) level for the zero point vibrational energy (ZPE)

Structure	D_e	ZPE	D_0
K9K9-1	8543	−265	8278
K9K7-2	7823	−331	7492
K9K7-1	7668	−259	7409
K7K7-2	7258	−329	6929
K7K7-1	6981	−257	6724
K9K9-3	6199	−332	5867
K7K7-4	6140	−420	5720
K9K7-3	5741	−306	5435
K9K9-5	5175	−567	4608
K9K9-6	5122	−528	4594
K9E9-1	5897	−418	5479
K9E9-2	5559	−546	5013
K9E9-3	4668	−365	4303
K9E9-4	4627	−327	4300
K9E9-5	4628	−331	4297
E9E9-1	5116	−360	4756
E9E9-2	4976	−294	4682
E9E9-3	4879	−389	4490
E9E9-4	4689	−300	4389
E9E9-5	4660	−310	4350
E9E9-6	4496	−367	4129
K9KM9-1	8559	−243	8316
K7KM9-2	7746	−342	7404
K9K7M1-2	7776	−376	7400
KM9K7M1	7743	−362	7382
K7KM9-1	7641	−260	7381
K7K7M1-2	7161	−351	6810

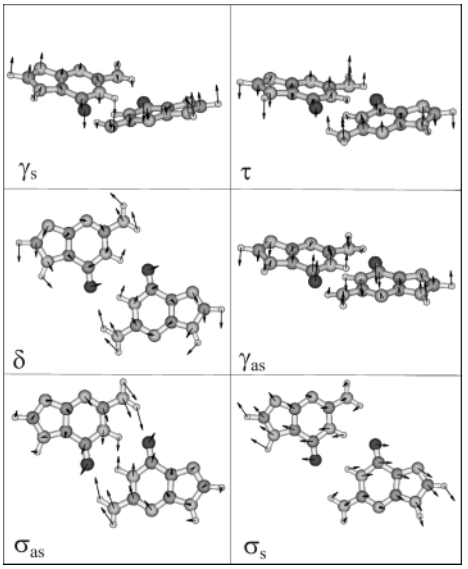

Fig. 2 Scheme of the intermolecular vibrations of the K9K7-1 dimer. These are the out-of-plane bending (butterfly) motion γ_s with the two guanine moieties as wings, the out-of-plane torsion or twisting motion τ, the in-plane bending (gearing) δ of the two moieties, the antisymmetric out-of-plane bending (alternating stairs) motion γ_{as} and the antisymmetric and symmetric stretching vibrations σ_{as} and σ_s.

Table 2 Harmonic frequencies (in cm^{-1}) and approximate descriptions of the intermolecular vibrations in the S_0 state of the most stable guanine dimers at the HF/6-311G(d,p) level. The 6 intermolecular vibrations originating from the three lost rotations and translations after dimerisation are the butterfly γ_s, torsion τ and gearing δ of the two rings, antisymmetric out-of-plane bending (step motion of the two moieties) γ_{as}, antisymmetric stretching (in-plane bending of the two monomer moieties) σ_{as} and symmetric stretching vibrations σ_s.

	γ_s	τ	δ	γ_{as}	σ_{as}	σ_s	D_0
K9K9-1	4	31	57	42	75	112	8278
K9K7-1	15	33	56	62	72	109	7409
K9KM9-1	7	31	54	44	74	110	8316
K9K7-2	13	27	87	47	76	112	7492
K7K9M-2	12	25[a]	75	44	80	110	7404
K9K7M1-2	12	25	76	46	80	106	7400
KM9K7M1	12	22a	75	43	80	104	7382

[a] Coupled with methyl torsion.

rotations and translations of the two monomers that are lost after dimerization. The intermolecular modes of the other guanine dimers look basically the same, however their frequencies and sometimes even their sequence differ considerably, *cf.* Table 2. Fig. 3 shows the OH- and NH-stretching vibrations of K9K7-1. Table 3 lists the harmonic frequencies (in cm^{-1}) of the OH and NH stretching vibrations in the S_0 state of the most stable guanine dimers at the HF/6-31G(d,p) level. We shall compare the experimental and the calculated vibrational frequencies below

UV–UV double resonance

Using UV–UV double resonance spectroscopy, we checked the R2PI spectra for different isomers of the guanine dimer and its methylated derivatives. The results are presented in Fig. 4. When scanning the burn laser with the analysis laser set to the red-most band of GG at 33103 cm^{-1} we observed that the intense band at $0+179$ cm^{-1} was missing in the hole burning spectrum. Hence we used that transition for analysis and

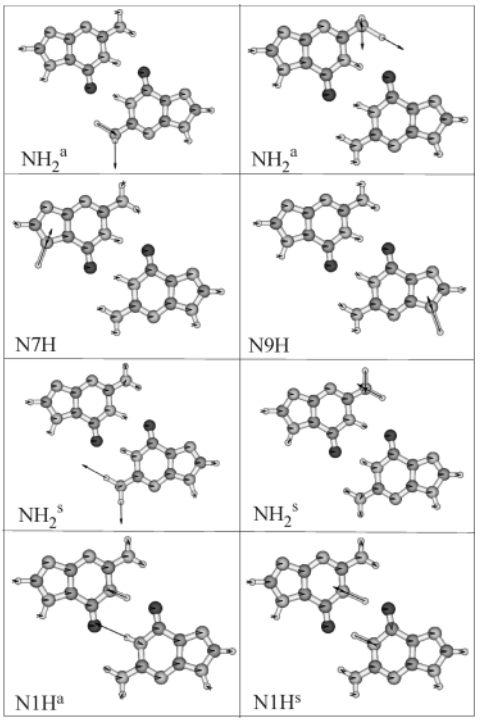

Fig. 3 Scheme of the high frequency normal mode vibrations of the K9K7-1 dimer. NH_2^a and NH_2^s label the antisymmetric and symmetric NH_2 stretching vibrations, respectively. N9H, N7H and N1H indicate the N9-H, N7-H and N1-H stretching vibrations.

scanned the burn laser again. In this way all R2PI transitions in the wavelength range from 32565 to 33600 cm^{-1} could be assigned to one of two isomers, which we shall denote as GG1 and GG2. Fig. 4 shows the R2PI and UV–UV hole burning spectra of these two GG isomers. For G-G1M(1-methylguanine), G-G9M(9-methylguanine) and G1M-G9M we observed only one isomer, *cf.* Fig. 4. A closer inspection shows that the vibronic spectra of GG1 and GG2 are quite different, especially in the region of the low frequency vibrations, which are most sensitive to the hydrogen bonded structure. On the other hand the vibronic patterns of G-G1M and GG1 resemble each other quite closely as do those of G-G9M and GG2. A methyl group in position 1 blocks the formation of the enol tautomer and hence of enol–enol dimers and of keto–keto and keto–enol dimers like K9K9-1, K9K7-1, K9E9-1, K9E9-2, K9E9-3 but allows cluster structures like K9K7-2 or K7K7-2. These findings will be important for the structural analysis presented later.

IR–UV double resonance

Fig. 5 presents the IR–UV double resonance spectra of guanine and methyl substituted guanine tautomers and their dimers, allowing comparison of their spectral patterns. Again we notice the close resemblance between the spectra of G-G1M and GG1 and between the spectra of G-G9M and GG2, respectively. In fact, the GG2 and G-G9M spectra are almost exactly equal except for the N9H stretching vibration, which appears in the GG2 spectrum at 3506 cm^{-1} and which is absent in G-G9M due to the methyl substitution at the N9 position. Likewise, the GG1 and G-G1M spectra are almost exactly equal except for the N1H stretching vibration, which appears in the GG1 spectrum at 3441 cm^{-1} and which is absent in G-G1M due to the methyl substitution at the N1 position. Furthermore the antisymmetric NH_2 stretching vibration of the 1-methyl substituted guanine is shifted in the cluster from 3530 to 3554 cm^{-1} in good agreement with the

Table 3 Harmonic frequencies (in cm^{-1}) and approximate descriptions of the OH and NH stretching vibrations in the S_0 state of the most stable guanine dimers at the HF/6-31G(d,p) level. Calculated frequencies are scaled with 0.893 obtained from comparison with the experimental guanine monomer frequencies.[4] The labels a and b indicate cluster moieties a and b in Fig. 1 where the vibration is predominantly located. NH_2^a and NH_2^s are the antisymmetric and symmetric NH_2 stretching vibrations. OH and 1H are the OH and N1-H stretching vibrations respectively.

	OH		NH_2^a		N9-H/N7-H		1H		NH_2^s		
Keto–keto	a	b	a	b	a	b	a	b	a	b	D_0
K9K9-1			3563	3563	3501	3501	3251	3226	3430	3429	8278
K9K7-2			3529	3542	3501[a]	3504	3450	3275	3253	3374	7492
K9K7-1			3555	3561	3513[a]	3501	3231	3259	3427	3432	7409
K7K7-2			3523	3537	3502[a]	3513[a]	3450	3257	3282	3382	6929
K7K7-1			3551	3551	3511	3511	3261	3238	3427	3427	6724
K9K9-3			3535	3551	3496	3506	3447	3277	3422	3406	5867
K7K7-4			3511	3511	3319[a]	3306[a]	3452	3452	3405	3405	5720
K9K7-3			3536	3542	3496	3514[a]	3446	3278	3423	3406	5435
K9K9-5			3516	3505	3324	3500	3448	3279	3409	3398	4608
K9K9-6			3517	3491	3473	3500	3448	3226	3309	3386	4594
Keto–enol											
K9E9-1	3685		3539	3555	3499	3503		3302	3343	3425	5479
K9E9-2	3370		3493	3545	3502	3502		3278	3389	3413	5013
K9E9-3	3476		3580	3525	3501	3501		3279	3451	3413	4303
K9E9-4	3427		3575	3535	3500	3365		3449	3448	3409	4300
K9E9-5	3392		3575	3520	3500	3470		3450	3448	3327	4297
K9E9-6	3368		3537	3510	3502	3488		3449	3424	3318	3622
Enol–enol											
E9E9-1	3388	3410	3575	3574	3500	3504			3448	3449	4756
E9E9-2	3334	3300	3571	3571	3503	3503			3447	3446	4682
E9E9-3	3452	3444	3572	3572	3501	3501			3446	3445	4490
E9E9-4	3697	3390	3576	3574	3352	3500			3447	3446	4389
E9E9-5	3698	3393	3574	3574	3358	3501			3444	3447	4350
E9E9-6	3697	3360	3556	3572	3467	3501			3391	3446	4129
G-GM											
K9KM9-1			3563	3564	3501		3251	3226	3430	3429	8316
K7KM9-2			3528	3542	3501[a]		3450	3274	3253	3375	7404
K9K7M1-2			3540	3567	3504	3503[a]	3256		3368	3266	7400
K9MK7M1-2			3541	3565		3503[a]	3258		3368	3280	7382
K7KM9-1			3559	3555		3513[a]	3261	3228	3431	3426	7381

[a] N7–H.

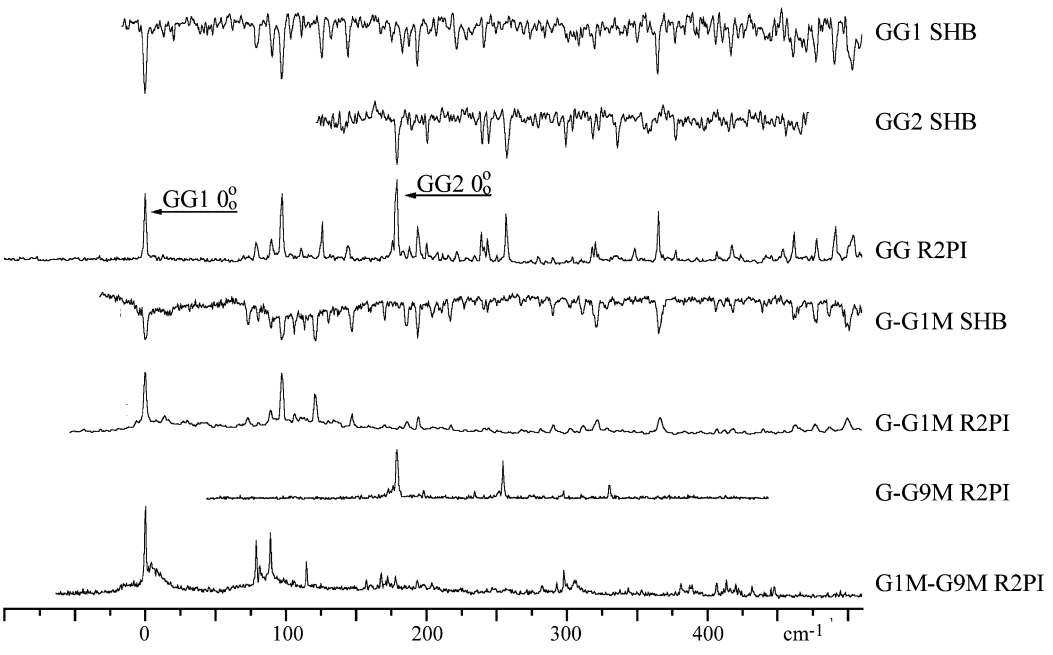

Fig. 4 R2PI and UV-UV hole burning spectra of the two GG isomers GG1 and GG2, G-G1M(1-methylguanine), G-G9M(9-methylguanine) and G1M-G9M. The electronic origins are at 33103 cm^{-1}(GG1), 33282 cm^{-1}(GG2), 33058 cm^{-1}(G-G1M), 33282 cm^{-1}(G-G9M) and 33622 cm^{-1}(G9M-G1M). The vibronic patterns of G-G1M and GG1 and of G-G9M and GG2 resemble quite closely.

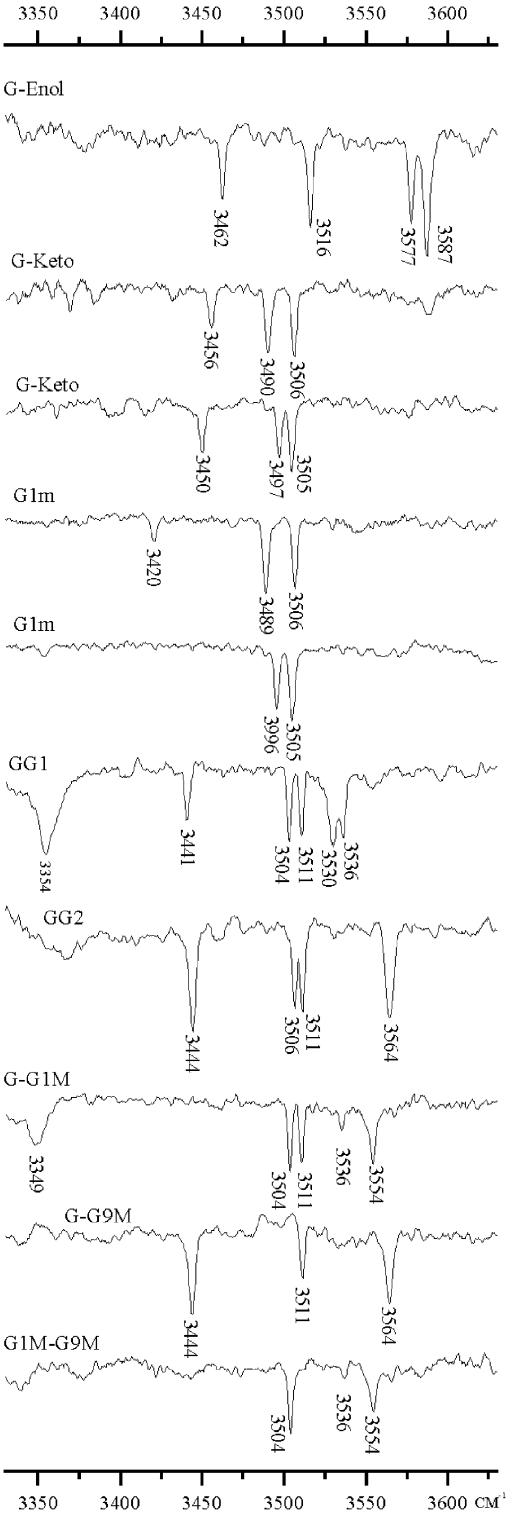

Fig. 5 IR–UV double resonance spectra of the guanine and methyl substituted guanine tautomers and their dimers. From top to bottom: guanine tautomer 1 (enol) analysed at 32870 cm^{-1}, guanine tautomer 2 (keto) analysed at 33275 cm^{-1}, guanine tautomer 3 (keto) analysed at 33914 cm^{-1}, methyl substituted guanine G1M analysed at 33628 cm^{-1} (keto tautomer 1 of 1-methylguanine), methyl substituted guanine G1M analysed at 32941 cm^{-1} (keto tautomer 2 of 1-methylguanine), guanine dimer GG1 analysed at 33103 cm^{-1}, guanine dimer GG2 analysed at 33282 cm^{-1}, methyl substituted guanine dimer G-G1M analysed at 33058 cm^{-1}, methyl substituted guanine dimer G-G9M analysed at 33282 cm^{-1}, methyl substituted guanine dimer G1M-G9M analysed at 33622 cm^{-1}. The IR band at 3536 cm^{-1} in G-G1M and G1M-G9M has a low intensity because for these two spectra we used an IR crystal with a gap in that region.

calculations to be presented below. The G1M-G9M spectrum resembles the G-G1M spectrum with a missing N9H stretching vibration.

IV Discussion

Fig. 6 compares the IR–UV spectra of the two isomers of the guanine dimer with the calculated vibrational frequencies of the most stable keto–keto dimers. We first compare the GG2 spectrum with the calculated spectra. The K9K9-1 spectrum has only three bands in the investigated spectral region from 3300 to 3700 cm^{-1}. Due to the high symmetry of this structure the corresponding vibrations in the cluster moieties couple but only the combinations of opposite phase are allowed, *i.e.* NH_2^a–NH_2^a, N9H–N9H, NH_2^s–NH_2^s. The corresponding + combinations are strictly forbidden. The N1H–N1H vibration is shifted to lower frequencies outside the investigated range due to the strong C=O···N1H/N1H···O=C hydrogen bonds. Hence the calculated spectrum shows only three bands in the investigated range in obvious contradiction to the experimental results.

The question arises why do we not observe this most stable isomer? The high (C_{2h}) symmetry of K9K9-1 leads to exciton splitting with two energy levels: (i) an S_0–S_1 transition at lower energy, which is forbidden because the transition dipoles are antiparallel, and (ii) an S_0–S_2 transition at higher energy, which has parallel transition dipoles and is thus allowed. The TD-DFT calculations on K9K9-1 indeed showed that the $S_1 \leftarrow S_0$ ($1A_g \leftarrow 1A_g$) transition has an oscillator strength of zero while the $S_2 \leftarrow S_0$ ($1B_u \leftarrow 1A_g$) transition is allowed. Red shifts of the optical dimer transitions relative to the monomer transitions are expected if the hydrogen bonds are more stable in the excited state than in the ground state and blue shifts if they are less stable. We expect shifts and splittings similar to the 2-pyridone dimer $(2PY)_2$ which also has symmetrical C=O···NH/NH···O=C hydrogen bonds and C_{2h} symmetry. The S_0–S_2 origin band of $(2PY)_2$ is at 30776 cm^{-1} while the 2PY monomer absorbs at 29831 cm^{-1} (a second conformer absorbs at 29928 cm^{-1}).[19,20] We expect similar large shifts in K9K9-1 which would cause the allowed S_0–S_2 transition to lie outside the spectral range investigated up to now.

K9K7-1 exhibits the same H bond arrangement as K9K9-1 but consists of 9H-/7H-keto moieties such that the exciton splitting is less and the S_0–S_1 transition is allowed. The six NH stretching vibrations of K9K7-1 have quite different frequencies and at first inspection the number of bands seems to be too large. However the NH_2^a frequencies of the 9H-/7H keto monomers are 3531/3513 cm^{-1} at the HF/6-31 G(d,p) level, respectively, while the experimental frequencies are 3506/3505 cm^{-1}. Therefore we infer that the HF calculations overestimate the frequency difference of the two NH_2^a vibrations. For K9K7-1 the calculated frequencies are 3561/3555 cm^{-1}. It is reasonable to assume that this frequency difference is also overestimated by the HF calculations and that thus the frequencies are actually closer together. We attribute the broad and weakly split band of GG2 at 3564 cm^{-1} to these two vibrations. Notice the blue shift of the NH_2^a vibrations of K9K7-1 compared to the monomer frequencies. We also found this shift for a number of other stretching vibrations of NH_2 groups involved in hydrogen bonds, *cf.* Table 3. The experiment also shows blue shifts of the NH_2^a vibrations, *cf.* the IR spectra of the two G-keto tautomers and GG1/GG2 in Fig. 5. The frequency difference of the N9H/N7H stretching vibrations is described quite well by the HF calculations with calculated values of 3501/3505 cm^{-1} for the monomer compared to experimental values of 3490/3497 cm^{-1}. We assign the GG2 bands at 3506/3511 cm^{-1} to these two NH stretching vibrations of K9K7-1.

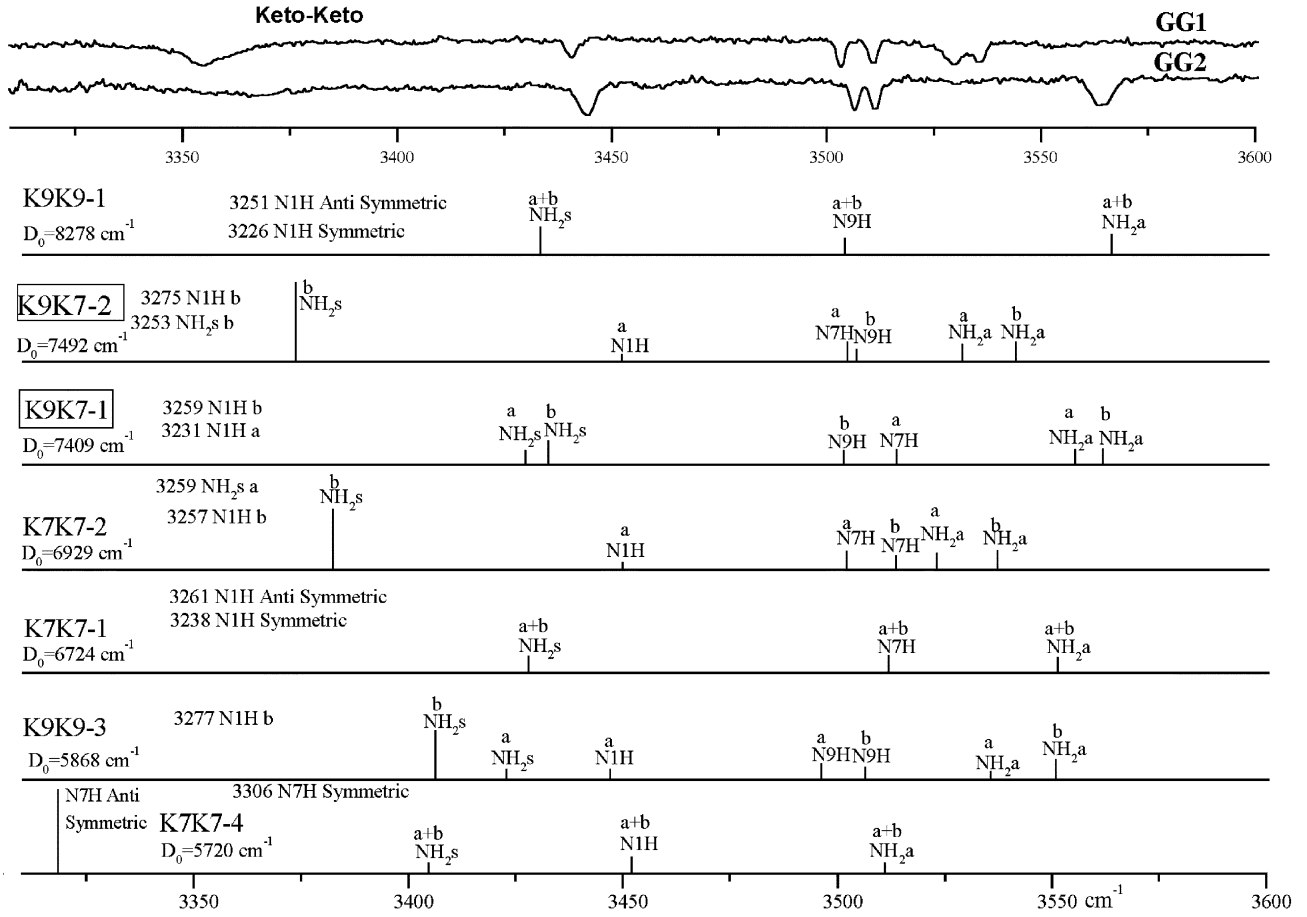

Fig. 6 The infrared spectra (IR–UV SHB) of the two isomers of the guanine dimer. The vibrational frequencies of the most stable keto–keto dimers calculated at the HF/6-31G(d,p) level are shown for comparison. The calculated frequencies are scaled by a factor 0.893 obtained from the best fit of the guanine monomer frequencies to the frequencies calculated at the HF/6-31G(d,p) level.

Further evidence for structural assignment of GG2 comes from the experiments with methylated guanine. As already discussed, the G-G9M vibronic spectra are very similar to the GG2 spectrum, and this is true for the respective IR spectra as well. Indeed the only difference is the N9H stretching vibration at 3506 cm^{-1}, which is missing in the 9-methyl substituted dimer (Fig. 10). The broad band at 3444 cm^{-1} can be assigned to the two NH_2^s vibrations with calculated frequencies of 3432/3427 cm^{-1} (9H/7H). The 9H/7H NH_2^s monomer frequencies are calculated to 3421/3407 cm^{-1}, in other words there is a 10–20 cm^{-1} red shift of these NH_2^s dimer vibrations when they are involved in hydrogen bond interactions. Experimentally we only observe the NH_2^s vibration in 1-methylguanine(9H)—in the other spectra of the keto monomers its activity is too small. Assuming that its frequency of 3420 cm^{-1} is similar in K9, the assignment of the band at 3444 cm^{-1} to NH_2^s is in qualitative agreement with the calculated blue shift of the NH_2^s vibration of K9K7-1. The N1H stretching vibrations are involved in strong hydrogen bonds in K9K7-1. According to the calculations they absorb at lower frequencies than experimentally investigated, *cf.* Fig. 6. Indeed GG2 exhibits no IR absorption in the region from 3320 to 3440 cm^{-1} where GG1 shows a broad and intense band as expected for a stretching vibration involved in a hydrogen bond. The other keto–keto IR spectra are in considerably poorer agreement with the experimental spectrum. From the remaining clusters only the K9E9-2 (Fig. 7) and E9E9-1 (Fig. 8) spectrum resemble the GG2 spectrum somewhat but they show too many bands in the low frequency region. We note however that the calculations may underestimate the strength of the OH···N,O hydrogen bonds in these clusters so that the corresponding H donor OH vibrations absorb at lower frequencies than experimentally accessible. However, it is reasonable to assign GG2 to structure K9K7-1, based on its large stability and the good agreement between its experimental and theoretical IR spectra. The question arises: why do we not see two electronic transitions in the unsymmetrical K9K7-1 dimer? The TD-DFT calculations showed that the $S_1 \leftarrow S_0$ transition (essentially a HOMO → LUMO transition with both orbitals mainly localised on K7) has a similar oscillator strength to the monomers while the the $S_2 \leftarrow S_0$ transition is 10 times weaker (essentially a HOMO-1 (mainly localised on K9) → LUMO (mainly localised on K7) excitation leading to a small transition electron density). This localisation of the frontier orbital coefficients was observed to be essentially independent of the basis sets used.

The GG1 spectrum agrees best with the K9K7-2 spectrum. The vibrations at 3536/3530, 3511/3504, 3441 and 3354 cm^{-1} can be assigned to the two NH_2^a vibrations involved in $NH_2\cdots N$ and $NH_2\cdots O{=}C$ hydrogen bonds, the N9H/N7H stretching vibrations, the N1H stretching vibration not involved in a hydrogen bond and NH_2^s involved in $NH_2\cdots N$ hydrogen bonding, respectively. This assignment is supported by the G-G1M spectrum shown in Fig. 5 and 9. Here the stretching vibration of the N1H group not involved in the hydrogen bonding is missing at 3441 cm^{-1} due to the methyl substitution in position 1. Beyond that the NH_2^a vibration adjacent to the methyl group shifts from 3530 cm^{-1} in GG1 to 3554 cm^{-1} in

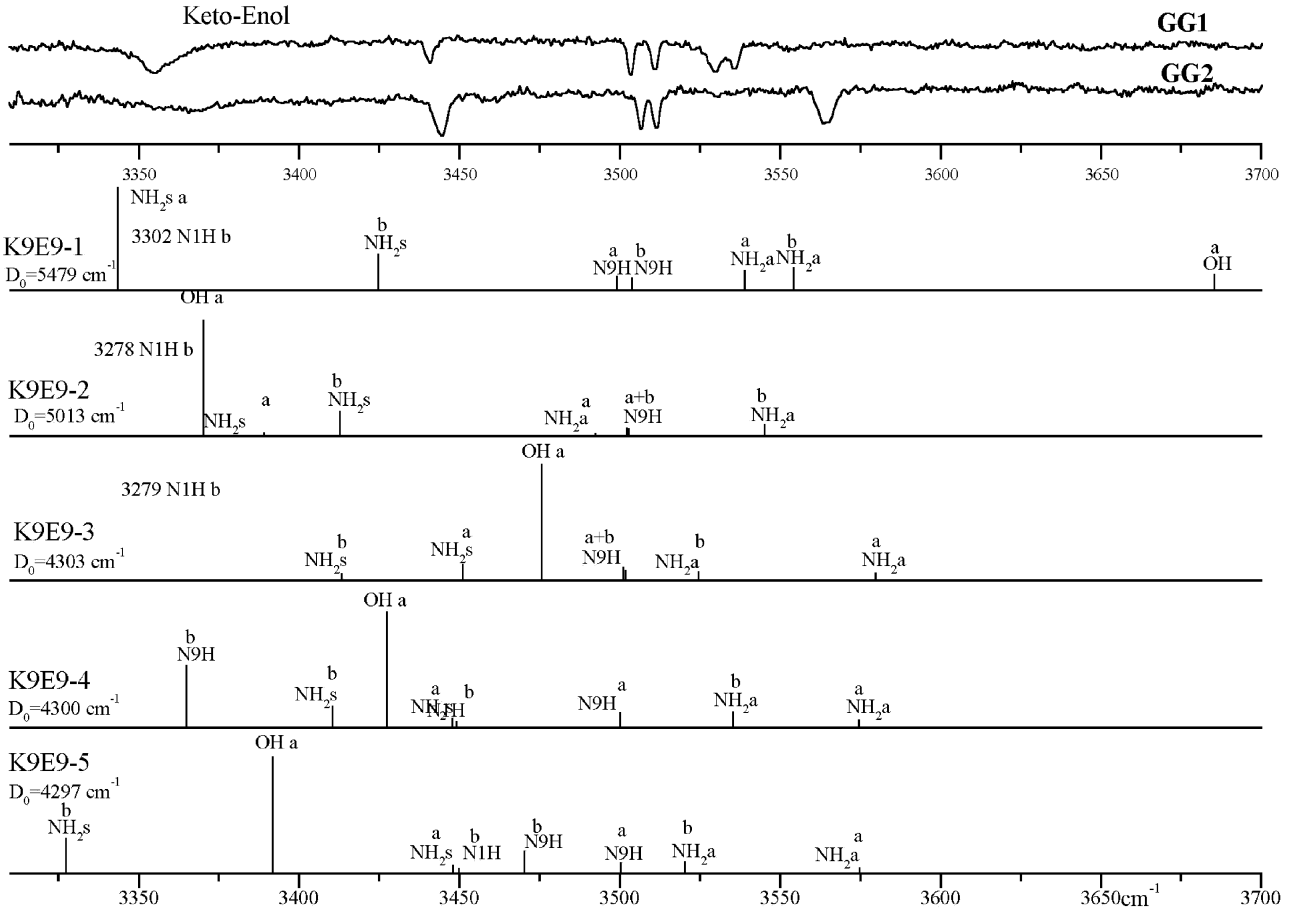

Fig. 7 The infrared spectra (IR–UV SHB) of the two isomers of the guanine dimer. The vibrational frequencies of the most stable keto–enol dimers calculated at the HF/6-31G(d,p) level are shown for comparison. The calculated frequencies are scaled by a factor 0.893 obtained from the best fit of the guanine monomer frequencies to the frequencies calculated at the HF/6-31G(d,p) level.

G-G1M in good agreement with the calculated frequencies displayed in Fig. 9 and Table 3 while the other $NH_2{}^a$ vibration stays unchanged at 3535 cm^{-1}. The G1M-G9M spectrum shown in Fig. 11 resembles the G-G1M spectrum merely the N9H stretching vibration being missing. Neither the G-G1M nor the G1M-G9M spectra can be associated to structures with a symmetrical C=O···N1H/N1H···O=C hydrogen bond arrangement because of the methyl substitution in position 1 but can hydrogen bond *via* HNH···N, NH···N and O=C··· HNH interactions, cf. KM9K7M1-2 in Fig. 1.

Hence the IR spectra with the methylated guanine dimers further support the assignment of GG1 to structure K9K7-2. The IR spectrum calculated for K7K7-2 shows nearly equally spaced $NH_2{}^a$ and N7H vibrational frequencies which do not match the GG1 spectrum as well. Furthermore the binding energy of this cluster is considerably lower than the K9K7-2 stabilization and the formation of mixed K9K7 dimers is statistically favoured by a factor of 2 because K9K7 and K7K9 dimers are formed equivalently. The other keto–keto, keto–enol and enol–enol spectra exhibit an even considerably poorer match with the experimental IR spectrum. Hence we assign the GG1 spectrum to structure K9K7-2. We did not observe any R2PI spectra of G1M-G1M which shows that at least one N1H position has to be available for cluster formation, supporting our assignment of the two spectra. Table 4 summarizes the comparison of experimental and theoretical NH frequencies for the assigned guanine dimers. Again the question arises why do we not see two electronic transitions in the unsymmetrical K9K7-2 dimer? According to the TD-DFT calculations the $S_1 \leftarrow S_0$ transition is very weak (essentially a HOMO (localised on K9) → LUMO (localised on K7) excitation) while the the $S_2 \leftarrow S_0$ transition has a similar oscillator strength to the monomers (essentially a HOMO-1 → LUMO transition with both orbitals localised on K7). Hence it is possible that in both dimers we merely observe the K7 excitation.

Table 5 lists the experimental electronically excited state intermolecular vibrational frequencies of GG1 and GG2 and a preliminary assignment based on the assumption that the calculated ground state intermolecular frequencies also reflect the sequence of vibrations in the excited state. Moreover the assignment is entirely based on spectroscopic arguments like plausible allocations of overtones and combination bands. Because, however, high quality electronically excited state vibrational frequencies are currently not available, the intermolecular vibrations in the electronically excited state state are not as suitable for structural assignment yet as the S_0 state OH and NH stretching vibrations

V Summary

Our UV–UV and IR–UV double resonance measurements of the guanine dimer and its methylated derivatives in the range 32565 to 33600 cm^{-1} reveal two isomers of the guanine dimer. From our findings a consistent picture emerges. We calculated 39 G–G structures. The dimer K9K9-1 has the largest binding energy but we did not observe it, probably due to its strong exciton splitting and hydrogen bond shift leading to the

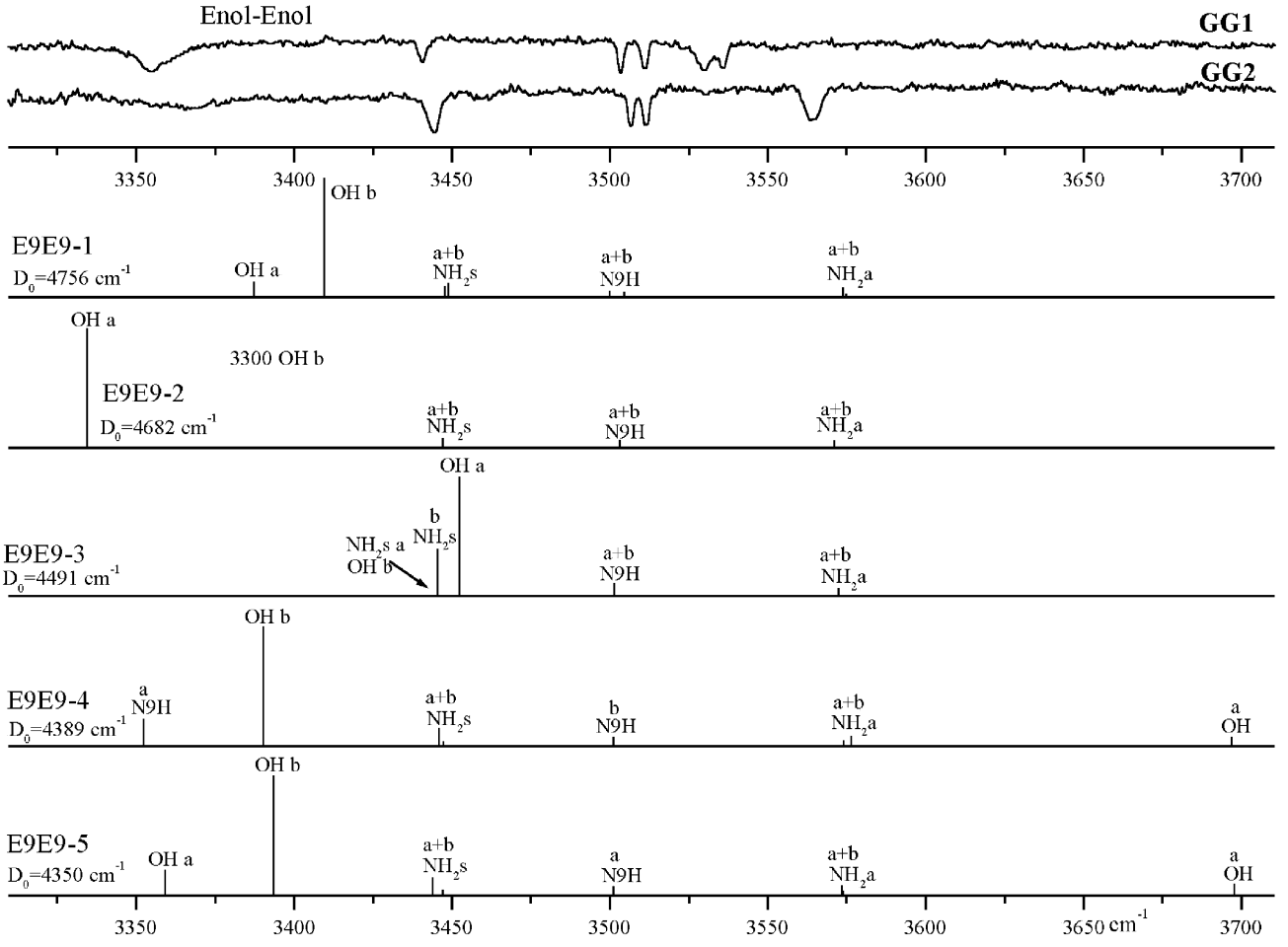

Fig. 8 The infrared spectra (IR–UV SHB) of the two isomers of the guanine dimer. The vibrational frequencies of the most stable enol–enol dimers calculated at the HF/6-31G(d,p) level are shown for comparison. The calculated frequencies are scaled by a factor 0.893 obtained from the best fit of the guanine monomer frequencies to the frequencies calculated at the HF/6-31G(d,p) level.

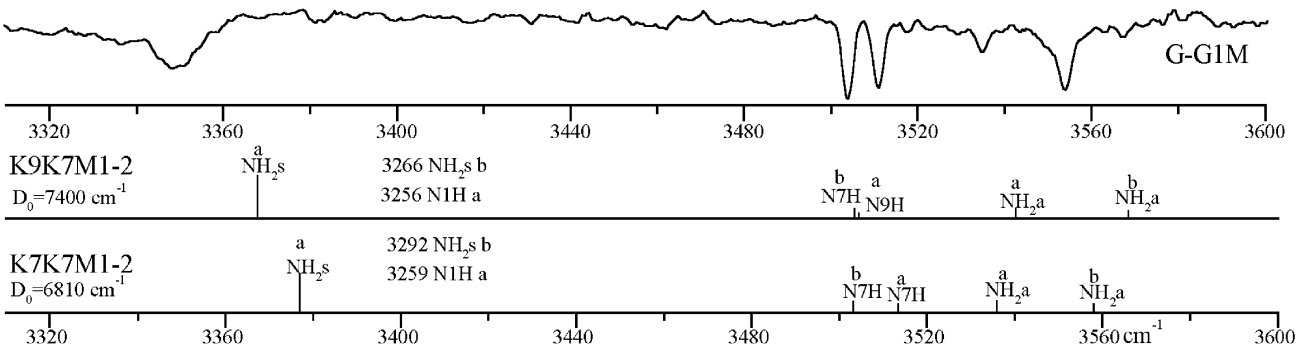

Fig. 9 The infrared spectrum (IR–UV SHB) of the methyl substituted guanine dimer G-G1M. The vibrational frequencies of the most stable G-G1M tautomers calculated at the HF/6-31G(d,p) level are shown for comparison. The calculated frequencies are scaled by a factor 0.893 obtained from the best fit of the guanine monomer frequencies to the frequencies calculated at the HF/6-31G(d,p) level.

allowed S_0–S_2 transition lying outside the investigated spectral range. We instead observed the next most stable GG isomers with three nonsymmetrical and two symmetrical H bonds, respectively. They are both mixed dimers consisting of 9H- and 7H-keto tautomers of guanine as cluster moieties so that statistics further favor their formation. We could not detect any keto–enol or enol–enol dimers in the investigated wavelength region. According to the calculations they are considerably less stable. We cannot exclude however that minor bands or bands in other wavelength regions belong to other isomers of the guanine dimer.

Acknowledgements

This work has been supported by the Deutsche Forschungsgemeinschaft, the "Regionales Rechenzentrum der Universität Köln" and the Israel Science Foundation, founded by the Israel Academy of Sciences and Humanities.

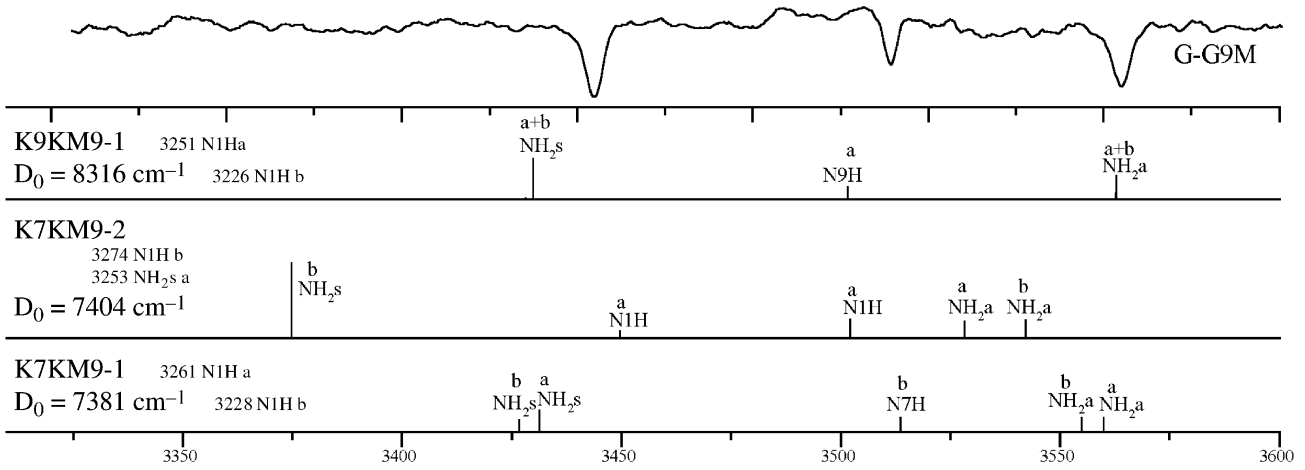

Fig. 10 The infrared spectrum (IR–UV SHB) of the methyl substituted guanine dimer G-G9M. The vibrational frequencies of the most stable G-G9M tautomers calculated at the HF/6-31G(d,p) level are shown for comparison. The calculated frequencies are scaled by a factor 0.893 obtained from the best fit of the guanine monomer frequencies to the frequencies calculated at the HF/6-31G(d,p) level.

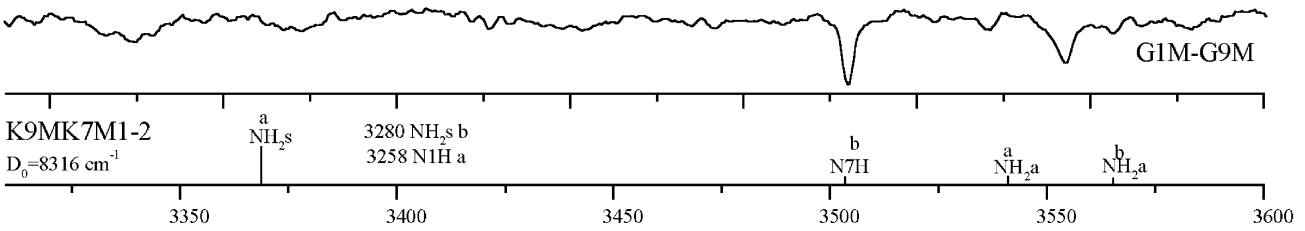

Fig. 11 The infrared spectrum (IR–UV SHB) of the methyl substituted guanine dimer G1M-G9M. The vibrational frequencies of the most stable G9M-G1M tautomer calculated at the HF/6-31G(d,p) level is shown for comparison. The calculated frequencies are scaled by a factor 0.893 obtained from the best fit of the guanine monomer frequencies to the frequencies calculated at the HF/6-31G(d,p) level.

Table 4 Vibrational assignments of the ground state fundamentals of the different isomers of the guanine dimer in the range of the OH and NH stretching vibrations. Calculated frequencies are scaled by 0.893, obtained from comparison with the experimental guanine monomer frequencies.[4] The labels (a) and (b) indicate cluster moieties a and b in Fig. 1 where the vibration is predominantly located. All values in cm^{-1}

	HF/6-31G(d,p) (K9K7-1)	Experiment (GG2)	HF/6-31G(d,p) (K9K7-2)	Experiment (GG1)
NH_2^a (b)	3561	3564	3542	3536
NH_2^a (a)	3555	3564	3529	3530
N7H (a)	3513	3511	3501	3504
N9H (b)	3501	3506	3504	3511
NH_2^s (b)	3432	3444	3374	3354
NH_2^s (a)	3427	3444	3253	—
N1H (b)	3259	—	3275	—
N1H (a)	3231	—	3450	3441

Table 5 Vibrational assignments of the excited (S_1) state intermolecular vibrations of the guanine dimers. The displayed theoretical intermolecular frequencies are calculated for the S_0 state. The experimental assignment is based on the assumption that the calculated order of the six fundamental intermolecular vibrations is not changed in the S_1 state. All values in cm^{-1}

	HF/6-31G(d,p) (K9K7-1)	Experiment (GG2)	HF/6-31G(d,p) (K9K7-2)	Experiment (GG1)
γ_s	15	21	13	—
τ	33	—	27	—
δ	56	60	87	90
γ_{as}	62	—	47	—
σ_{as}	72	65	76	78
σ_s	109	78	112	97
$\tau+\tau$				103
$\gamma_{as}+\gamma_{as}$				111
$\delta+\delta$		120		
Unassigned				125
$\delta+\sigma_{as}$		125		
$\gamma_{as}+\tau$				132
$\delta+\sigma_s$		139		
$\sigma_{as}+\sigma_s$		144		175
$\delta+\gamma_{as}$				144
$\sigma_s+\sigma_s$		157		
$\sigma_s+\sigma_s+\tau$		178		
$\sigma_{as}+\tau+\tau$				182
$\delta+\sigma_s$				187
$\delta+\tau+\tau$				193
$\delta+\delta+\sigma_s$		198		

References

1 E. Henderson, C. C. Hardin, S. K. Walk, I. Tinoco and E. H. Blackburn, *Cell*, 1987, **51**, 899.
2 R. J. Wellinger and D. Sen, *Eur. J. Cancer*, 1997, **33**, 735.
3 A. Gualberto, R. M. Patrick and K. Walsh, *Genes Develop.*, 1992, **6**, 815.
4 J. L. Battiste, M. Hongyuan, N. Sambasiva Rao, T. Ruoying, D. R. Muhandiram, L. E. Kay, A. D. Frankel and J. R. Williamson, *Science*, 1996, **273**, 1547.
5 P. Hobza and J. Sponer, *Chem. Rev.*, 1999, **99**, 3247.
6 J. Sponer, J. Leszczynski and P. Hobza, *J. Phys. Chem.*, 1995, **100**, 1965.
7 M. Elstner, P. Hobza, T. Frauenheim, S. Suhai and E. Kaxiras, *J. Chem. Phys.*, 2001, **114**, 5149.
8 E. Nir, K. Kleinermanns and M. S. de Vries, *Nature*, 2000, **408**, 949.
9 E. Nir, C. Janzen, P. Imhof, K. Kleinermanns and M. S. de Vries, *J. Chem. Phys.*, 2001, **115**, 4604.

10 G. Meijer, M. S. de Vries, H. E. Hunziker and H. R. Wendt, *Appl. Phys. B*, 1990, **51**, 395.
11 R. K. Frost, F. Hagemeister, D. Schleppenbach, G. Laurence and T. S. Zwier, *J. Phys. Chem.*, 1996, **100**, 16835.
12 R. N. Pribble, C. Gruenloh and T. S. Zwier, *Abstr. Pap. Am. Chem. Soc.*, 1996, **211**, 176.
13 M. Schmitt, H. Muller and K. Kleinermanns, *Chem. Phys. Lett.*, 1994, **218**, 246.
14 W. Scherzer, H. L. Selzle and E. W. Schlag, *Chem. Phys. Lett.*, 1992, **195**, 11.
15 S. Ishikawa, T. Ebata, H. Ishikawa, T. Inoue and N. Mikami, *J. Phys. Chem.*, 1996, **100**, 10531.
16 M. J. Frisch, G. W. Trucks, H. B. Schlegel, P. M. W. Gill, B. G. Johnson, M. A. Robb, J. R. Cheeseman, T. Keith, G. A. Petersson, J. A. Montgomery, K. Raghavachari, M. A. Al-Laham, V. G. Zakrzewski, J. V. Ortiz, J. B. Foresman, J. Cioslowski, B. B. Stefanov, A. Nanayakkara, M. Challacombe, C. Y. Peng, P. Y. Ayala, W. Chen, M. W. Wong, J. L. Andres, E. S. Replogle, R. Gomperts, R. L. Martin, D. J. Fox, J. S. Binkley, D. J. Defrees, J. Baker, J. P. Stewart, M. Head-Gordon, C. Gonzalez and J. A. Pople, Gaussian Revision A.4, Gaussian, Inc., Pittsburgh, PA, 1995.
17 M. Kabelá and P. Hobza, *J. Chem. Phys., B*, 2001, **105**, 5804.
18 M. Mons, personal communication, 2001.
19 A. Held, B. B. Champagne and D. W. Pratt, *J. Chem. Phys.*, 1991, **95**, 8732.
20 Y. Matsuda, T. Ebata and N. Mikami, *J. Chem. Phys.*, 1999, **110**, 8397.